IEEE Transactions on Nuclear Science, Vol.NS-22, No.3, June 1975

TESTS ON S-BAND SUPERCONDUCTING NIOBIUM PROTOTYPE ACCELERATOR STRUCTURES*

P. Kneisel†, C. Lyneis and J. P. Turneaure

Department of Physics and High Energy Physics Laboratory

Stanford University, Stanford, California 94305

Summary

The fabrication, processing, and measurement of two S-band niobium prototype electron accelerator structures are discussed. Maximum surface magnetic fields were typically between 250 and 350 Oe, corresponding to average energy gradients between 4.6 and 6.5 MeV/m, with Q_o values typically greater than 3×10^9. The structures which were electropolished gave more reproducible results than those which were chemically polished.

Introduction

Measurements on single-cell TM_{010} mode niobium cavities at X-band, S-band, and L-band made at Stanford[1-3] and elsewhere,[4-5] have shown that the maximum field which can be attained increases with operating frequency. Although this information indicated that it may be desirable to operate the Stanford superconducting linac in a higher frequency band than L-band, experience has shown that experimental results for single-cell cavities may not be simply extended to results for large multi-cell structures,[6-7] since they have yielded field values well below those attained for single-cell cavities. For these reasons, two seven-cell S-band niobium prototype accelerator structures were built and tested.

Structure Design

A schematic drawing of the seven-cell S-band structure is shown in Fig. 1. The structure which is designed to operate at 2.85 GHz is basically a scaled-down version of the capture section for the Stanford superconducting accelerator which operates at 1.3 GHz.[6] The structure consists of five cells of length 0.5λ which are between the end cells of length 0.35λ, and it operates in the standing-wave π mode in the lowest TM_{01} band. The axial electric field profile is flat in the π mode except in the center cell where it is 3/4 that of the other cells. The rf and accelerator properties of the structure are given in Table I. The average energy gradient, which includes transit time effects, is calculated assuming a particle of one unit of electronic charge and with velocity c.

Table I
RF and Accelerator Properties of π-Mode Structure

Frequency	2.85 GHz
Length	0.337 m
Geometric Factor	260 Ω
Shunt Impedance/QL	1900 Ω m^{-1}
Peak Surface Magnetic Field / $(\omega \times \text{Stored Energy})^{\frac{1}{2}}$	3.98×10^{-3} Oe $W^{-\frac{1}{2}}$
Peak Surface Magnetic Field / Average Energy Gradient	54 Oe $(MeV)^{-1}$
Peak Surface Electric Field / Average Energy Gradient	3.6 MV $(MeV)^{-1}$

Structure Fabrication

The fabrication techniques used for the S-band structures are similar to those used for the L-band structures.[6] The S-band structures are fabricated as follows: (1) reactor-grade niobium sheet of about 5mm thickness is cut into round blanks, (2) the round blanks are die-formed into cups each of which form one-half a cell, (3) the die-formed cups are vacuum stress relieved at 975°C for 1 hour, (4) the stress-relieved

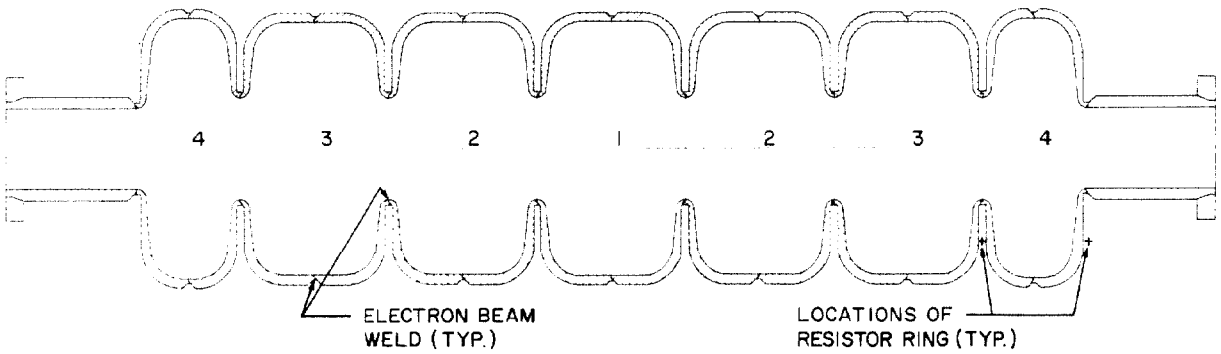

Figure 1. Schematic drawing of the seven-cell S-band structure. Numbers indicate different cell types.

* Work supported by the National Science Foundation under Grant GP 39029.

† Present address: Institut fur Experimentelle Kernphysik, Kernforschungszentrum, Karlsruhe, W. Germany.

cups are machined to final dimensions, (5) the completed cups are joined with 100% penetration electron-beam (EB) welds to form the seven-cell structure, (6) to give the structure rigidity and to support it in the ultra-high vacuum (UHV) furnace, three niobium support bars are EB welded to the exterior of the structure, and (7) the structure is rotated about its axis with 6 mm diameter ball bearings in all cells to remove any niobium spatter produced during EB welding. A photograph of the completed structure after fabrication and some processing is shown in Fig. 2.

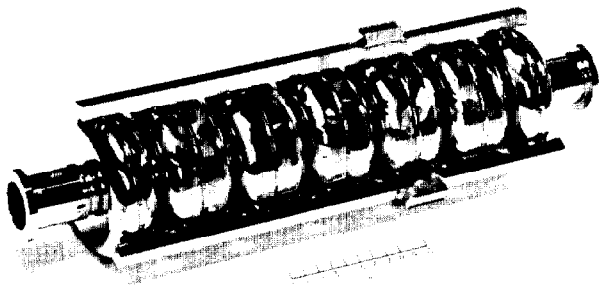

Figure 2. Photograph of an S-band structure.

Structure Processing and Assembly

The structures were processed using a number of techniques which included chemical polishing, electropolishing, anodizing, oxipolishing, rinsing and UHV firing. The initial processing of both structures and the details of the processing techniques are described below. The processing steps subsequent to the initial processing are given in Table II.

The initial processing of the two structures involved different surface cleaning procedures. For structure No. 1, the surface was cleaned by immersing the structure in a solution of 3 parts HF (70% solution), 2 parts concentrated HNO_3 and 5 parts H_2O at 22°C followed by rinsing in distilled water and methanol. For structure No. 2, the surface was cleaned by electropolishing with the removal of 9μm and then by oxipolishing. After the initial surface cleaning, both structures were UHV fired at 1800°C for 10 hours.

Chemical polishing was done by immersing the structure vertically into a solution of 2 parts HF (40% solution) and 3 parts concentrated HNO_3 at -10 to -5°C. This solution removes niobium at about the rate of 5μm/min.

Electropolishing was done by immersing slightly more than one-half of the structure, whose axis was horizontal, in a solution of 85 parts concentrated H_2SO_4 and 10 parts HF (40% solution) at a temperature of 25°C and by then applying a constant voltage in the range of 10 to 15V. The voltage and temperature were adjusted until good current oscillations were observed. The typical electropolishing cycles consisted of two steps while the structure rotated at 20°/min: (1) 1.5 min of polishing with the voltage on and (2) 5.5 min of solution circulation with the voltage off. One electropolishing cycle removes about 1μm of niobium

Anodizing was done by immersing the structure in a 1% solution of NH_4OH and slowly raising the voltage to 100V over a time period of 10 to 20 min to keep the current approximately constant.

Oxipolishing was done by alternately anodizing the structure and then stripping the oxide layer in a 70% solution of HF. This process was typically repeated twice, and then a final oxide layer was placed on the structure by anodizing.

Rinsing procedures depended on the sequence of chemical and electrochemical treatments. Between treatments the structure was always rinsed in distilled water. After all chemical and electrochemical treatments were completed, the final cleaning steps were (1) rinsing in distilled water, (2) rinsing in methanol and (3) drying in filtered nitrogen gas.

UHV firing of the structure, which was always the final processing step prior to assembly, was done in an UHV furnace at 1800°C for 3 to 10 hours. The typical pressure in the furnace at the firing temperature was in the low 10^{-5} torr range, and this pressure decreased about a decade during cooldown.

After the final firing of a structure for a given test, the structure was assembled using indium gaskets to an rf probe and to a pumping line for evacuating the structure. In all but the first test of structure No. 1 (test 1 - 1) the assembly took place in a glove box filled with a dry nitrogen atmosphere. The rf probe provided a fixed coupling as well as a low temperature ceramic rf vacuum window. The structure was evacuated with an UHV pumping system; and, after it was evacuated to 10^{-8} torr or less, a copper tubulation was pinched off to remove the structure from the UHV pumping system. In test 1 - 1, the structure was assembled to an adjustable rf probe which also served as the pumping line to which a 2ℓ/s sputter-ion pump was attached at room temperature. The adjustable rf probe assembly could reach about 10^{-7} torr when the structure was at room temperature.

Measurement Methods

The low temperature tests were made in a magnetically shielded dewar where the ambient field was ≤ 1mOe and the operating temperature was about 1.5 K. The tests included measurements of the rf characteristics, the rf breakdown position, and the radiation produced. Usually the rf measurements included the low and high power Q_o's and the maximum attainable field for each of the seven modes in the TM_{01} band. Some of the early measurements were limited to the π mode and the modes nearby in frequency because of limited rf equipment. To locate the cell in which breakdown occurred, a system was developed for detection of the heat pulse produced during breakdown. Eight teflon rings, each having thirteen 56Ω resistors in series mounted on them, were attached to the structure such that the rings of resistors were located adjacent to the highest magnetic field regions of the cells as indicated in Fig. 1. This method of localizing the breakdown gives a clear determination of the cell where breakdown occurs. X-radiation measurements were typically made with an ionization type radiation meter.

Measurement Results and Discussion

Table II is a summary of measurement results for all twelve tests on S-band structure No. 1 (SS-1) and S-band structure No. 2 (SS-2). For each test, it includes the low power Q_o, the maximum surface electric and magnetic field attained, the Q_o and x-radiation level at the maximum field, and appropriate comments; as well as the surface treatment prior to each test. Both structures attained maximum surface fields of about 355 Oe and 25 MV/m, which corresponds to an average energy gradient of 6.5 MeV/m, with Q_o's at this

Table II

Results of S-Band Structure Tests Operated in π Mode

Structure and Test	Q_o at Low Power	H_{max}(Oe) E_{max}(MV/m) on Surface	Q_o at H_{max}	Surface Treatment	Radiation (mR/hr at 1m)	Comments
1 - 1	4.3×10^8	113 7.3	2×10^8	50μm CP fired	ND	only experiment with adjustable probe
1 - 2	8.2×10^9	242 15.5	3×10^9	50μm CP anodized fired	ND	
1 - 3/4	1.6×10^{10}	356 23	4.5×10^9	50μm CP anodized fired	7	breakdown on bottom of lower No. 4 cell
1 - 5/6	1.6×10^9	$\gtrsim$ 41 $\gtrsim$ 2.6	1.1×10^8	75μm CP anodized fired	ND	low Q_o at high power & available RF power limited fields attained
1 - 7	4.6×10^9	176 11.4	7.5×10^9	50μm CP anodized fired	ND	leak in initial pinch-off, breakdown on top of lower No. 4 cell
1 - 8	1.15×10^{10}	260 16.8	7.7×10^9	50μm EP anodized fired	.05	breakdown on top of lower No. 4 cell
1 - 9	1.5×10^{10}	280 18.1	1.7×10^{10}	100μm EP oxipolished fired	.03	breakdown on bottom of center cell (No. 1)
1 - 10	1.15×10^{10}	300 19.4	1.4×10^{10}	50μm EP oxipolished fired	0.1	breakdown on top of lower No. 3 cell
2 - 1	1.8×10^{10}	290 18.7	2.45×10^{10}	100μm EP oxipolished fired	ND	breakdown on bottom of lower No. 4 cell
2 - 2	6.4×10^9	105 6.8	1.1×10^9	50μm EP oxipolished fired	ND	multipacting barrier limited field, breakdown on bottom of upper No. 3 cell
2 - 3	1.2×10^{10}	250 16.2	3.6×10^9	90μm EP oxipolished fired	$\gtrsim$ .1	breakdown on bottom of upper No. 3 cell
2 - 4	1.9×10^{10}	355 23	3.1×10^9	10-20μm CP anodized fired	$\gtrsim$ 5	breakdown on bottom of lower No. 4 cell

Legend: CP - Chemically Polished, EP - Electropolished and ND - Not Detected ($<$ 0.01mR/hr at 1m)

field level of 4.3×10^9 for SS-1 and 3.1×10^9 for SS-2. The twelve tests may be divided into those with "poor" performance and those with "good" performance. The three tests with "poor" performance, which included tests 1 - 1, 1-5/6 and 2 - 2, attained maximum magnetic fields of 113 Oe or less. For tests 1 - 1 and 1-5/6 the fields were limited by low Q_o's at the maximum fields, and for test 2 - 2 an electron-multipacting barrier in the upper No. 3 cell appeared to initiate thermal-magnetic breakdown. The remaining nine tests with "good" performance attained maximum magnetic fields in the range of 176 to 356 Oe. There is a correlation between the Q_o at the maximum field level and a "poor" or "good" performance. Those tests with "poor" performance have Q_o's of 1.1×10^8 to 1.1×10^9, and those with "good" performance have Q_o's of 3×10^9 to 2.4×10^{10}.

The reproducibility of structures processed by electropolishing appears to be superior to that of chemical polishing, at least as we practice these polishing techniques. For chemically polished structures; two out of six tests exhibited "poor" performance, and the four tests with "good" performance had maximum fields in the range of 176 to 356 Oe. For electropolished structures; one out of six tests exhibited "poor" performance, and the five with "good" performance had maximum fields in the range of 250 to

Table III

Breakdown and Q_o in TM_{01} Modes for Test 2-4

Mode	Frequency MHz	Low Power Q_o	High Power Q_o	Stored Energy (Joules)	Radiation mR/hr at 1m	Location of Breakdown
0	2727	5.1×10^{10}	4.0×10^{10}	.350	.06	Bottom of center cell (No. 1)
$\pi/6$	2743	4.8×10^{10}	1.8×10^{10}	.284	ND	Not located
$2\pi/6$	2758	5.4×10^{10}	0.72×10^{10}	.447	1.1	Not located
$3\pi/6$	2798	2.0×10^{10}	0.50×10^{10}	.295	2.1	Top of upper No. 2 cell
$4\pi/6$	2818	1.58×10^{10}	0.21×10^{10}	.309	3.2	Bottom of lower No. 4 cell
$5\pi/6$	2842	0.95×10^{10}	0.10×10^{10}	.226	4.0	Bottom of lower No. 4 cell
π	2849	1.50×10^{10}	0.31×10^{10}	.418	$\gtrsim 5.0$	Bottom of lower No. 4 cell

Legend: ND - Not Detected (< 0.01 mR/hr at 1m)

300 Oe. Although chemically polished structures resulted in the highest maximum fields, electropolished structures resulted in a higher percentage of tests with "good" performance and they resulted in maximum magnetic fields which were in a considerably narrower range.

A more complete summary of typical measurements made on all seven modes in the TM_{01} band of an S-band structure is given for test 2 - 4 in Table III. With the information in this table, one can examine the homogeneity of the superconducting surface since each of the seven modes has substantially different field profiles. In particular the homogeneity with respect to thermal-magnetic breakdown field can be examined. For example, experimental axial electric field profiles show that the field level in the No. 4 cells is at a maximum for the $4\pi/6$, $5\pi/6$ and π modes, and indeed thermal-magnetic breakdown is observed in the bottom of the No. 4 cell for each of these modes. The $3\pi/6$ mode has a maximum field in the No. 2 cells, and thermal-magnetic breakdown is observed at the top of the upper No. 2 cell. Likewise, the 0 mode has its maximum field in the center cell, and again thermal-magnetic breakdown is observed in the center cell. This information indicates that for test 2 - 4 the surface was relatively homogeneous with respect to its thermal-magnetic breakdown properties. However it should be pointed out that the surface was less homogeneous in other tests. For example, in test 1 - 7, thermal-magnetic breakdown occurred on the top of the lower No. 4 cell in all seven modes indicating a surface region in this cell which had a considerably lower thermal-magnetic breakdown field than in the other cells of the structure.

Conclusion

The S-band seven-cell prototype structures were built and tested to evaluate the performance of large S-band niobium structures relative to that of 6-m long L-band niobium structures which are used for the Stanford superconducting linac. A 3-m long S-band structure, which is composed of seven sub-structures (each with seven excited cells) and designed for 2.6GHz, has been fabricated and partially processed, and we expect to test it in May 1975. Because of the greater reproducibility of the seven-cell prototype structures when processed with electropolishing, the 3-m long S-band structure will be electropolished rather than chemically polished. One can make an approximate estimate of the performance of the 3-m long S-band structure based on the fact that it consists of seven sub-structures of about the same configuration as the seven-cell prototype structures. The maximum field of the 3-m long structure is determined by the lowest of the maximum attainable fields for the seven sub-structures, and its Q_o is determined by the average of the Q_o's for the seven sub-structures. Since five out of six prototype structure tests using electropolishing gave "good" performance, one can expect a moderate probability for the 3-m long structure of attaining a maximum field of 250 Oe, corresponding to an average energy gradient of 4.6 MeV/m, and a Q_o of 1.3×10^{10}. These values may be compared with the highest average energy gradient and Q_o attained in a 6-m long L-band structure[6] which are 3.8 MeV/m and 6.9×10^9. The improved reproducibility of the electropolished S-band prototype structures indicates that it is worthwhile applying the electropolishing technique to the 6-m L-band structures.

References

1. J. P. Turneaure and Nguyen Tuong Viet, Appl. Phys. Letters 16, 33 (1970).
2. J. P. Turneaure, IEEE Trans. Nucl. Sci. NS-18, 166 (1971).
3. C. Lyneis, M. McAshan and Nguyen Tuong Viet, Proc. of 1972 Proton Linear Acc. Conf. (Los Alamos Scientific Lab., 1972), p. 98.
4. H. Martens, H. Diepers and B. Hillenbrand, Phys. Letters 44A, 213 (1973)
5. P. Kneisel, O. Stoltz and J. Halbritter, J. Appl. Phys. 45, 2502 (1974).
6. J. P. Turneaure, H. A. Schwettman, H. D. Schwarz and M. S. McAshan, Appl. Phys. Lett. 25, 247 (1974).
7. W. Bauer, A. Citron, G. Dammertz, M. Grundner, L. Husson, H. Lengler and E. Rathgeber, Proc. of 9th Int. Conf. on High Energy Acc. (SLAC, 1974), p. 133.
8. H. Diepers, O. Schmidt, H. Martens and F. S. Sun, Phys. Letters 37A, 139 (1971).